Turbulent Liquid-Liquid Dispersion in Sulzer SMX Mixer

Félicie Theron, Nathalie Le Sauze, Alain Ricard

Turbulent Liquid−Liquid Dispersion in Sulzer SMX Mixer

Félicie Theron,* Nathalie Le Sauze, and Alain Ricard

LGC, Laboratoire de Génie Chimique, Université de Toulouse, 4 Allée Emile Monso, BP 84234, 31432 Toulouse Cedex 4, France

This paper presents an experimental study of pressure drop of single-phase flow and liquid−liquid dispersion through a Sulzer SMX mixer in the turbulent flow regime. Emulsification experiments are performed with various numbers of mixing elements from 2 to 20 and different flow rates ranging from 204 to 600 L/h. Pressure drop in single phase flow when *Re* is greater than 800 is modeled using a correlation based on the Blasius approach. The pressure drop is quantified at high Reynolds numbers for a liquid−liquid system. The droplet size distribution evolves along the mixer, and 10 mixing elements are required to reach break-up coalescence equilibrium in the case of emulsification experiments. Finally, assuming Kolmogorov's theory of isotropic turbulence, a new correlation is established to predict the Sauter mean diameter in this mixing device as a function of the Reynolds and Weber numbers as well as the number of mixing elements.

1. Introduction

Liquid−liquid dispersions find many applications as emulsified products such as cosmetics, pesticides, or drugs, but also as intermediate steps in different processes (extraction, separation, polymerization). Reactions inside droplets or at their interface enable the control of the size distribution of final products. For all of these reasons, research in the frame of liquid−liquid dispersions is an active field of investigation as it concerns many industrial applications. In the recent context of process intensification, the use of static mixers is an interesting alternative to classical mechanical stirrers. They integrate perfectly in continuous processes and enable energy costs to be reduced.

Motionless mixers consist of fixed structures inserted into cylindrical pipes. As many designs are available, they must be selected according to required performances. Liquid−liquid dispersion in static mixers is achieved by passing the two immiscible liquids cocurrently through the mixers. As frictional forces are more uniform in static mixers compared to rotational stirrers, the equilibrium between breakage and coalescence is reached more quickly.

The energy cost also depends on the mixer type and is represented by the power needed by pumps to move the fluid through the mixer. This energy consumption can be estimated through pressure drop, and this parameter must be controlled and well-known to predict the size of droplets generated by the mixer.

Many studies have been carried out on pressure drop in static mixers in single phase flow. However only little information about pressure drop in liquid−liquid dispersion is available in the open literature. Moreover, most studies on SMX mixers have been performed in the laminar regime.[1,2] The turbulent flow was studied by Li et al.,[3] Pahl and Muschelknautz,[4−6] Bohnet et al.,[7] and Streiff et al.,[8] but, except in the work reported by Li et al.,[3] the experimental conditions needed for comparisons have not been detailed.

Liquid−liquid dispersion in turbulent flow has been performed in different mixer designs by many authors. The performance of the Kenics mixer has been investigated by Middleman,[9] Chen and Libby,[10] and Berkman and Calabrese.[11] Streiff[12] used the SMV mixer, Matsumura et al.[13] used the Hi-Mixer, Al Taweel and Walker[14] worked with the Lightnin design, Al Taweel and Chen[15] reported results obtained using woven screens, Lemenand et al.[16−18] used the high efficiency vortex (HEV) mixer, and recently Yamamoto et al.[19] compared the performances of three types of mixer: the needle jetting mixer (NJM), the Kenics mixer (KSM), and the Raymond supermixer (RSM). Some results about emulsification performance in turbulent flow in a SMX static mixer were reported by Streiff et al.[20] and Legrand et al.[21] Finally, Hirschberg et al.[22] showed some results about the use of a new kind of SMX mixer. Thakur et al.[23] published a review about the use of static mixers for mixing of miscible fluids, heat transfer, and interface generation for liquid−liquid and gas-systems.

The aim of this paper is to investigate the ability of the SMX mixer for liquid−liquid dispersion in turbulent flow. After having correlated the pressure drop obtained in single-phase flow, the pressure drop is quantified at high Reynolds number for a liquid−liquid system. Then the droplet size distribution of the liquid−liquid dispersion is determined and correlated in terms of mean energy dissipated according to Kolmogorov's (see Hinze[24,25]) theory of isotropic turbulence.

2. Experimental Section

2.1. Fluids Used. The hydrodynamics of the SMX mixer has been characterized through pressure drop acquisitions in single-phase flow. To cover a wide range of Reynolds numbers, four Newtonian fluids have been used: 40 wt % water−60 wt % glycerol (Gaches chimie), 60 wt % water−40 wt % glycerol, 98.5 vol % water−1.5 vol % Tween 80 (Panréac), and cyclohexane (Acros Organics). The properties of these fluids are summarized in Table 1. Viscosities were measured with an AR2000 rheometer (TA Instruments).

For liquid−liquid dispersion experiments, the fluids used were water and Tween 80 (surfactant, 1.5% vol) as the continuous phase and cyclohexane as the dispersed phase. The interfacial tension between cyclohexane and 1.5% vol Tween 80 water solution was measured by the Wilhelmy plate analysis using a Balance 3S (GBX Instruments) tensiometer and was equal to 3 mN/m.

2.2. Experimental Rig and Procedure. Figure 1 shows the schematic diagram of the experimental rig. The apparatus comprises a stainless steel tube packed with Sulzer SMX static

* To whom correspondence should be addressed. E-mail: Felicie.Theron@ensiacet.fr. Tel: +33 (0)5 34 32 36 72. Fax: +33 (0)5 34 32 36 00.

Table 1. Experimental Conditions for Pressure Drop Acquisition in Single-Phase Flow

fluids	water−glycerol (60% weight)	water−glycerol (40% weight)	cyclohexane	water−Tween 80 (1.5% vol)
density (kg/m^3)	1143	1090	770	995
viscosity (Pa•s)	0.0083	0.0032	0.0009	0.0010
range of flow rate $Q \times 10^6$ (m^3/s)	16.7−94.4	20.8−97.2	34.7−61.1	34.7−125
Re	274−1555	848−3959	1387−5985	4129−14865

mixer elements (see Figure 2), with a diameter of 10 mm. The aspect ratio *D*/*L* of each element was 1, and the porosity ε was 0.67. The number of mixing elements aligned in the tube was respectively 5, 10, and 15 for the pressure drop acquisition in single phase flow, and 2, 5, 10, 15, and 20 for the liquid−liquid dispersion.

The dispersed phase entered the cylindrical tube containing SMX mixers through a small tube, characterized by a 6 mm and 4 mm outer and inner diameter, respectively.

2.3. Data Acquisition. Pressure drops generated by the SMX mixer have been measured using a differential pressure gauge (Rosemount).

Droplets size distributions have been analyzed using a Mastersizer 2000 (Malvern Instruments). Before each measurement, an appropriate dilution of samples into continuous phase (water−Tween 80 1.5% vol) has been made in order to respect the obscuration range fixed in the apparatus procedure.

3. Results and Discussion

3.1. Pressure Drop in Single-Phase Flow. 3.1.1. Experimental Results. Although static mixers offer interesting features for mixing or dispersing two immiscible fluids, they also generate high pressure drops compared to empty pipes. As a consequence, the use of static mixers requires high energy input. Therefore, it is crucial to be able to predict the pressure drop for the respective flow regime concerned by the operation. Moreover the knowledge of pressure drop is necessary to predict the efficiency of the mixer, for example to calculate the mean droplet diameters in liquid−liquid dispersion applications.

The four different fluids mentioned above have been used to obtain experimental data covering a wide range of Reynolds numbers, especially under turbulent flow regime ($300 < Re < 14\,900$). For each fluid, two parameters have been considered: the number of mixing elements n_e (5, 10, and 15) and the fluid flow rate *Q*. Fluid properties and flow rate ranges are given in Table 1.

Figures 3−6 show data points obtained for the four fluids tested. As expected, the pressure drop increases with the number of elements. However, as shown in Figure 7 this increase is not proportional to the number of elements. The linear pressure drop is the highest for five elements, especially for the highest flow rates investigated, then levels off from 10 to 15 elements.

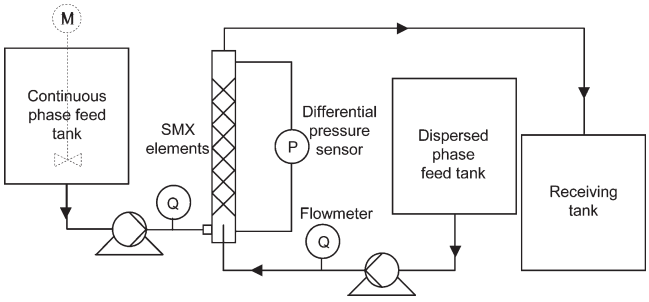

Figure 1. Schematic diagram of the experimental rig.

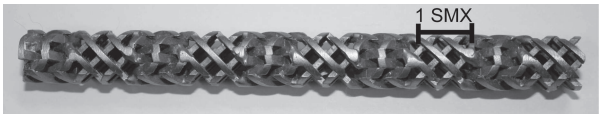

Figure 2. A set of 10 SMX elements.

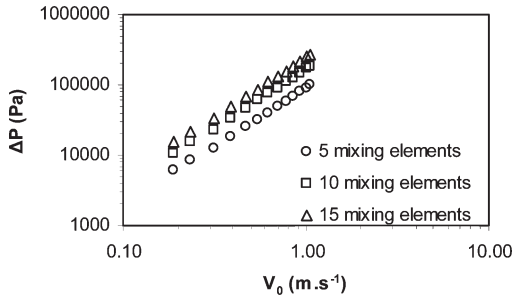

Figure 3. Influence of the number of mixing elements on the pressure drop for 40 wt % water−60 wt % glycerol solution.

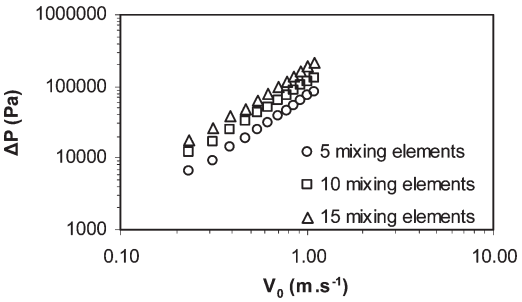

Figure 4. Influence of the number of mixing elements on the pressure drop for 60 wt % water−40 wt % glycerol solution.

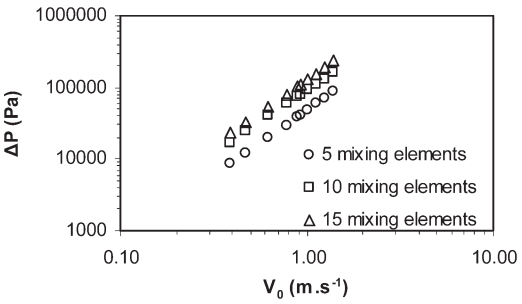

Figure 5. Influence of the number of mixing elements on the pressure drop for 98.5%(vol) water−1.5 vol % Tween80 solution.

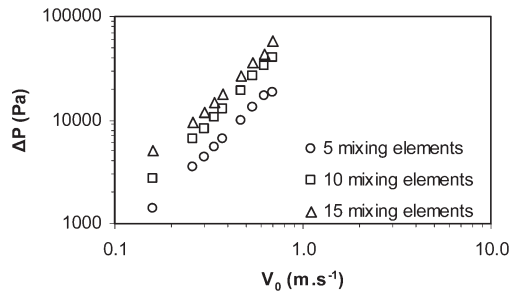

Figure 6. Influence of the number of mixing elements on the pressure drop for cyclohexane.

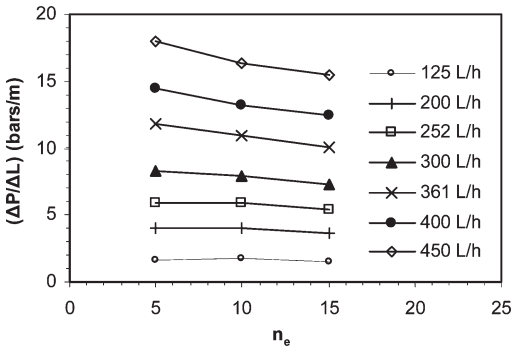

Figure 7. Influence of the flow rate on the linear pressure drop measured with cyclohexane.

The value of the pressure drop measured for five elements results from the linear pressure drop generated by the static mixer plus a singular pressure drop due to an entrance effect. This entrance effect is never mentioned in the literature. Its strong impact on pressure drop for five elements reported here may be due to the small size of the mixer tested. For 10 elements and more, this effect is no longer significant.

3.1.2. Correlation of Pressure Drop in Single-Phase Flow in SMX Mixers. Many correlations are available in the literature about pressure drop modeling in static mixers. These correlations are established for each design of static mixer. The most studied mixers are the Kenics and Sulzer SMX mixer. One way to correlate pressure drop in a static mixer ΔP_{SM} is to compare this value to the pressure drop in an empty pipe ΔP_{EP} of the same diameter and in the same conditions. The Z factor is usually employed:

$$Z = \frac{\Delta P_{SM}}{\Delta P_{EP}} \tag{1}$$

Another way of correlating pressure drop through static mixers is to determine the friction factor f or the Newton number Ne as a function of the Reynolds number Re. f and Ne are defined as followed:

$$Ne = 2f = \frac{\Delta P}{\rho V_0^2}\frac{D}{L} \tag{2}$$

where V_0 is the superficial velocity of the fluid, D the diameter of the tube, L the mixer length, and ρ the density of the fluid. These dimensionless numbers are usually correlated to the Reynolds number that can be calculated through the following expression, which is only valid for Newtonian fluids:

$$Re = \frac{\rho V_0 D}{\mu} \tag{3}$$

where μ is the viscosity of the fluid.

Several modified Reynolds numbers have been reported in the literature. Shah and Kale[1] also proposed a Reynolds number and a friction factor in terms of the interstitial velocity V_0/ε:

$$f_i = \frac{\Delta P D \varepsilon^2}{2L\rho V_0^2} \tag{4}$$

$$Re_i = \frac{\rho V_0 D}{\varepsilon \mu} \tag{5}$$

These expressions enable the comparison of mixers with different porosity.

Streiff et al.[8] defined a Reynolds number in terms of the hydraulic diameter of the mixer D_h and the interstitial velocity:

$$Re_h = \frac{\rho V_0 D_h}{\varepsilon \mu} \tag{6}$$

The expression of Shah and Kale[1] based on the interfacial velocity and the relation of Streiff et al.[8] in terms of the hydraulic diameter and the interstitial velocity are more appropriate than a relation based on the superficial velocity to compare mixers with different geometries. But most of the authors do not precise the geometric characteristics of their mixers and use a general approach where the Reynolds number is calculated in terms of the superficial velocity. Therefore, in the present paper this last approach is chosen in order to compare our results with results given in the literature.

Table 2 sums up correlations of pressure drop in the SMX mixer available in literature. Pahl and Muschelknautz[4−6] give Z factor values for laminar flow. Other Z values have been calculated from the correlations proposed and by determining the pressure drop in empty pipes from Bernoulli's equation for laminar flow:

$$\frac{f}{2} = \frac{8}{Re} \tag{7}$$

and from Blasius' correlation for turbulent flow:

$$\frac{f}{2} = \frac{0.0395}{Re^{0.25}} \tag{8}$$

If the pressure drop through the SMX mixer in laminar flow is quite well documented, there are few results available for turbulent flow, and the different correlations proposed for this regime are not equivalent.

Some authors, like Pahl and Muschelknautz,[5,6] consider that the Newton number is independent of the Reynolds number, which would correspond to fully developed turbulence. On the other hand, others find that the Newton number decreases with increasing Re. Li et al.[3] worked up to a Reynolds number equal to 10000. They set the beginning of turbulent flow at $Re = 1000$ and showed a decrease in the friction factor. The correlation used by these authors as well as by Bohnet et al.[7] to describe the turbulent flow indicates an exponent equal to -0.25 for the Reynolds number. This value corresponds to the Reynolds number exponent in the Blasius' model developed for empty pipes flows.

3.1.3. Correlation of Experimental Data. The global representation of experimental pressure drop values in terms of the friction factor as a function of the Reynolds number enables the identification of the limit between the transient and turbulent regimes through a change of the curve profile. From Figure 8, corresponding to experimental data obtained using four different fluids and three different mixer lengths, one can set the limit between the transition and turbulent flow at $Re = 800$.

The experimental results are correlated through an equation equivalent to the Blasius' model, likening the static mixers walls to a smooth duct. The correlation is determined for 10 elements, as the singular pressure drop due to the entrance effect becomes negligible from this number of elements. Moreover such a number of elements provides an appropriate representation of the industrial realty. The following expression has been obtained (cf. Figure 7):

$$\frac{f}{2} = \frac{24}{Re^{0.25}} \tag{9}$$

This relation correctly describes the turbulent regime for the SMX static mixer used. The pressure drop through the SMX mixer may also be compared to the pressure drop through empty pipes. The increase due to the mixing elements rises by a factor

Table 2. Correlations of Pressure Drop in SMX Mixer from the Literature

authors	SMX mixer characteristics	correlation	Z	Reynolds range
Pahl and Muschelknautz[4]	$D = 50$ mm; $L/D = 1.5$; 5, 7, 9 elements		10−100	$Re \leq 50$
Pahl and Muschelknautz[5,6]	$D = 50$ mm; $L/D = 1.5$; 5, 7, 9 elements	$Ne = 6$	10−60	$Re \leq 50$ $Re \geq 1000$
Bohnet et al.[7]	$D = 50$ mm	$\frac{f}{2} = \frac{236.6}{Re}$	30	$1.8 < Re < 20$
		$\frac{f}{2} = \frac{217.6}{Re} + 1.0$		$20 < Re < 1350$
		$\frac{f}{2} = \frac{9.1}{Re^{0.25}}$	230	$1350 < Re < 4000$
Shah and Kale[1]	$D = 26.54$ mm; $L/D = 1.5$; 24 elements; $\varepsilon = 0.87$	$f_i = \frac{350}{Re_i} + \frac{5.13}{Re_i^{0.58}}$		$Re_i < 10$ ($\approx Re < 10$)
Li et al.[3]	$D = 16$ mm; $L/D = 1.25$; 6, 8, 12 elements; $\varepsilon = 0.84$	$\frac{f}{2} = \frac{184}{\mathrm{Re}}$	23	$Re < 15$
		$\frac{f}{2} = \frac{110}{\mathrm{Re}^{0.8}} + 0.4$		$15 < Re < 1000$
		$\frac{f}{2} = \frac{6}{\mathrm{Re}^{0.25}}$	152	$1000 < Re < 10000$
Streiff et al.[8]		$Ne = \frac{1,200}{Re} + 5$	38	laminar: $Re_h < 20$ turbulent: $Re_h > 2300$
Yang and Park[2]	$D = 40$ mm; $L/D = 1$; 4, 8, 12 elements	$\frac{f}{2} = \frac{8.55}{Re^{1.61}}$		$Re < 20$

of $f_{SM}/f_{EP} = Z = \Delta P_{SM}/\Delta P_{EP} = 633$ with f_{SM} calculated using Blasius' equation. Such an additional energy cost may be justified if the use of static mixers enables us to reach specific results, for example in terms of droplet size in liquid−liquid dispersion.

3.1.4. Comparison with Existing Correlations. Figure 9 compares the correlation proposed for experimental data (i.e., the correlation based on Blasius equation) to the correlations established by different authors. Li et al.[3] identified the onset of the turbulent regime at $Re = 1000$, which is close to the value determined for the motionless mixers used in this study (Figure 9).

Streiff et al.[8] covered laminar, transient, and turbulent flow and set the beginning of turbulent flow at $Re_h = 2300$ what is equivalent in our case to $Re = 6700$, whereas we set the limit at $Re \approx 800$.

The pressure drops measured in this study are about 5 times higher than the values obtained by Li et al.[3] and 3 times higher than those reported by Bohnet et al.[7] This discrepancy may be due to the geometrical differences between the three SMX mixers used. Different porosities and hydraulic diameters may result in different pressure drops. As a consequence, correlations based on interstitial velocity and hydraulic diameter should be used in order to provide a better comparison between different mixers. Bohnet et al.[7] and Streiff et al.[8] do not precise these geometric parameters. Li et al.[3] specify the porosity of their mixer $\varepsilon = 0.84$, whereas the porosity of our mixer is 0.67.

A comparison between the present results and those reported by Li et al.[3] is proposed in Figure 10 where the friction factor and the Reynolds number are calculated from the interstitial velocity. Such a presentation of results enables us to take into account the different porosities of the mixers. The following model is obtained for the experimental data of the present work:

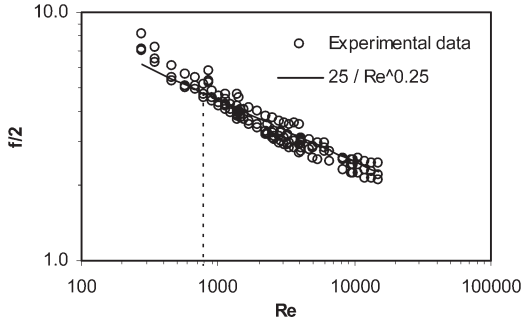

Figure 8. Correlation of 135 experimental data obtained under different conditions.

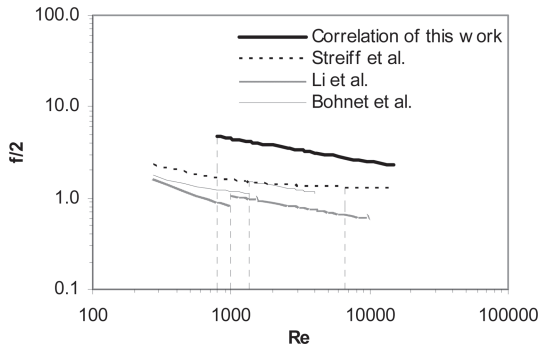

Figure 9. Comparison between the correlation proposed in this work and the different correlations available in the literature.

Table 3. Correlations Proposed by Different Authors to Calculate D_{32} or D_{43} in Different Conditions

authors	mixer design	characteristic diameter	Φ	equation	regime	α	β
Middleman[9]	Kenics	D	0.005−0.01	$\frac{D_{32}}{D} = K_4 We_c^{-0.6} Re^{0.1}$	turbulent	−0.6	0.1
Streiff[12]	Sulzer SMV	D_h	≤0.25	$\frac{D_{32}}{D_h} = 0.21 We_h^{-0.5} Re_h^{0.15}$	transient, turbulent	−0.5	0.15
Haas[30]	Kenics	D		$\frac{D_{43}}{D} = 1.2 We^{-0.65} Re^{-0.2} \left(\frac{\mu_d}{\mu_c}\right)^{0.5}$	laminar	−0.65	−0.2
Legrand et al.[21]	SMX	d_p	0.05−0.25	$\frac{D_{32}}{D_p} = 0.29 We_p^{-0.2} Re_p^{-0.16}$	laminar, transient and turbulent	−0.2	−0.16
Chen and Libby[10]	Kenics	D		$\frac{D_{32}}{D} = 1.14 We^{-0.75} \left(\frac{\mu_d}{\mu_c}\right)^{0.18}$	turbulent	−0.75	0
Matsumura et al.[13]	Hi Mixer	D	0.2	$\frac{D_{32}}{D} = K We_c^{-n} \qquad n = 0.56-0.67$	turbulent	−0.67to −0.67	0
Al Taweel and Walker[14]	Lightnin	D_h	0.01	$\frac{D_{32}}{D_h} = K We^{-0.6} f^{-0.4}$	turbulent	−0.6	
Berkman and Calabrese[11]	Kenics	D	<0.1	$\frac{D_{32}}{D} = 0.49 We^{-0.6} \left(1 + 1.38 Vi \left(\frac{D_{32}}{D}\right)^{0.33}\right)^{0.6}$	turbulent	−0.6	0
Al Taweel and Chen[15]	Woven Screens		0.01−0.04	$D_{32} = 0.682 (We_{jet}^{-0.859} \varphi^{0.875}) \left(\frac{b}{M}\right)^{0.833}$	turbulent	−0.859	0
Streiff et al.[20]	SMV, SMX, SMXL		0.01	$d = C_n (1 + K\varphi) \left(\frac{(1 + BVi) We_c}{2}\right)^{0.6} \left(\frac{\sigma}{\rho_c}\right)^{0.6} \left(\frac{\rho_c}{\rho_d}\right)^{0.1} \varepsilon^{-0.4}$ $d_{max} = 0.94 \left(\frac{\sigma}{\rho_c}\right)^{0.6} \varepsilon^{-0.4}$			
Lemenand et al.[16−18]	HEV	D	0.025−0.15	$\frac{D_{32}}{D} = 0.57 We^{-0.6}$	turbulent	−0.6	0
Das et al.[29]	SMX	D_p	0.05−0.25	$\frac{d_{max}}{d_p} = C We_p^{-0.33}$	laminar, transient	−0.33	0
Hirschberg et al.[22]	SMX plus		0.05	$d = C_n (1 + K\varphi) \left(\frac{(1 + BVi) We_c}{2}\right)^{0.6} \left(\frac{\sigma}{\rho_c}\right)^{0.6} \left(\frac{\rho_c}{\rho_d}\right)^{0.1} \varepsilon^{-0.4}$	turbulent		

$$\frac{f_i}{2} = \frac{12}{Re_i^{0.25}} \tag{10}$$

The correlation reported by Li et al.[3] is transposed in terms of Re_i and f_i, which gives

$$\frac{f_i}{2} = \frac{5.3}{Re_i^{0.25}} \tag{11}$$

The ratio between the numerators in the correlations obtained for the present work and that reported by Li et al.[3] is almost equal to 5 for the representation in terms of superficial velocity, and is equal to about 2 for the representation in terms of interstitial velocity. The difference in the ratios highlights the influence of porosity on the pressure drop and shows that it is essential to take into account the porosity in the correlations in order to satisfactorily compare different mixers.

However, the porosity does not explain the whole discrepancy between the results obtained in both cases discussed here. The hydraulic diameter should play a certain role. Moreover the diameter of the mixer used by Li et al.[3] is of 15 mm and its aspect ratio *L*/*D* is equal to 1.5, whereas the diameter of the mixer used for the work described here is of 10 mm, and its aspect ratio is equal to 1. Finally the smaller diameter of our mixer may create edge effects that could explain the higher pressure drops.

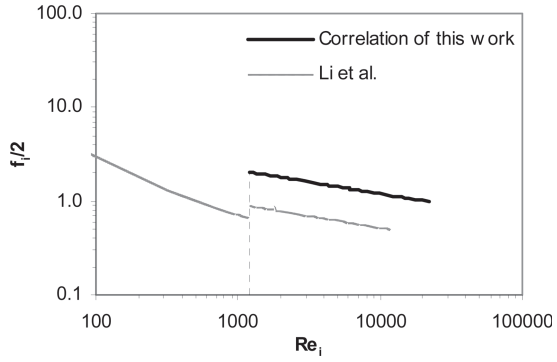

Figure 10. Comparison between the correlation proposed in this work and the correlation of Li et al.[3] in terms of the interstitial Reynolds number and the interstitial friction factor.

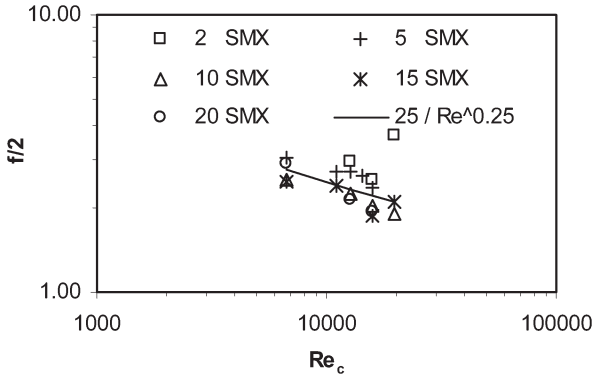

Figure 11. Comparison between liquid−liquid experimental values and correlations established with single-phase flow results.

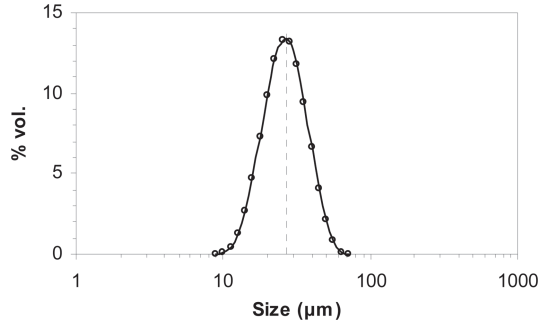

Figure 12. Droplet size distribution for a flow rate of 435 L/h, with n_e = 10 elements.

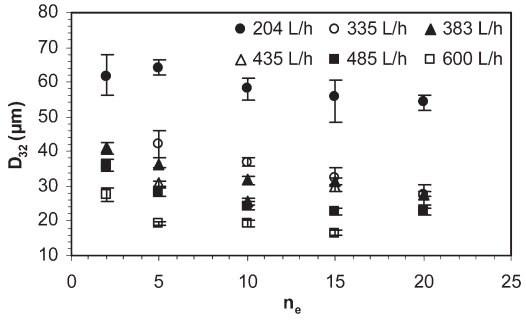

Figure 13. Evolution of D_{32} with the static mixer length at different flow rates (L = 0.1 m, what corresponds to n_e = 10).

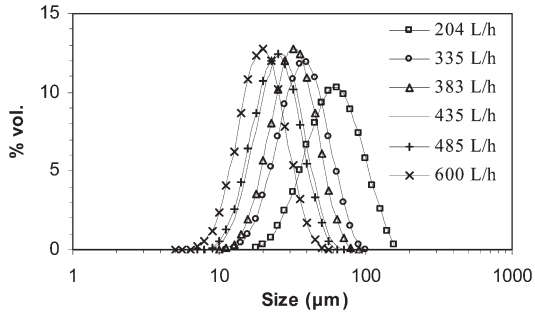

Figure 14. Effect of n_e on droplet size distribution for experiments at 485 L/h.

3.2. Pressure Drop in Liquid−Liquid Dispersion. For emulsification experiments, the parameters considered were the number of mixing elements n_e (2, 5, 10, 15, and 20) and the total flow rate Q (204−600 L/h). The concentration of the dispersed phase Φ was fixed to the value of 25% in volume and is defined as follows in terms of respective flow rates of each fluid:

$$\varphi = \frac{Q_d}{Q_c + Q_d} \tag{12}$$

Where Q_d and Q_c are the volume flow rate of the dispersed phase (cyclohexane) and the volume flow rate of the continuous phase (98.5% vol water−1.5% vol Tween80), respectively.

Figure 11 compares the experimental results with the correlation established in single-phase flow. Re_c is the Reynolds number calculated with the continuous phase properties. One can observe that the experimental results are in good agreement with the correlation based on the Blasius model when 10, 15, and 20 mixers are used. The higher pressure drops obtained with 2 and 5 SMX mixers are probably due to transient blockages of small interstices of the SMX porous medium by irregular drops of the dispersed phase, as suggested by Rama Rao et al.[26] When the equilibrium between breakage and coalescence is reached, the pressure drop in two-phase flow can be successfully modeled by the equation obtained in single-phase flow. For concentration lower than 50%, the viscosity of emulsions only varies slightly with the percent of dispersed phase. Straightforwardly, the pressure drops must be very similar for the monophasic system and for the emulsion studied here, allowing the use of the same model for both systems.

3.3. Liquid−Liquid Dispersion. 3.3.1. Droplet Size Distribution. Figure 12 shows an example of droplet size distribution where the volume fraction is plotted as a function of droplet size. The distributions follow a log-normal function and can be characterized by the Sauter mean diameter D_{32}:

$$D_{32} = \frac{\sum_i n_i d_i^3}{\sum_i n_i d_i^2} \tag{13}$$

where n_i is the number of droplets whith a size between d_i and d_{i+1}.

3.3.2. Effect of Number of Elements. Figure 13 illustrates the impact of the residence time (resulting from the number of elements, i.e. the mixer length) on the Sauter mean diameter for the total flow rate range (204−600 L/h).

For experiments performed at the lowest flow rate (i.e., 204 L/h), the droplet size distribution is broad and the resulting average size is high. Dispersions generated at this flow rate are quite unstable and opalescent, whereas other emulsions exhibit a rather opaque aspect.

The droplet size decreases as the number of mixing elements increases. This trend is more pronounced as flow rate decreases. Middleman[9] also reported the same effect of additional elements for the Kenics mixer on drop size.

Figure 14 shows droplet size distributions for experiments carried out at 485 L/h with different numbers of mixer elements. The Sauter mean diameter and the standard deviation become almost constant from 10 SMX elements. The same working number of elements is obtained for other flow rates.

At a given flow velocity, the mean energy dissipation rate per mass unit ε_v can be estimated through pressure drop measurement as follows:

$$\varepsilon_v = \frac{Q\Delta P}{L\frac{\pi D^2}{4}\varepsilon\rho_c} = \frac{Q\Delta P}{V_{app,mixer}\rho_c} \tag{14}$$

The mean energy dissipation rate per mass unit can be regarded as a measure of turbulence intensity at any point within the mixer. This assumption has been made by Al-Taweel and Walker[14] who worked on liquid−liquid dispersions using Lightnin mixers. They concluded that the addition of mixing elements does not alter the turbulence intensity at a given flow velocity but simply maintains the specific turbulence level. After fast drop break-up in the first elements (in our case: $0 < n_e < 5$), the break up phenomenon goes on as long as turbulence is maintained, and the average drop size is achieved when the dynamic equilibrium between break up and coalescence is reached. Higher fluid velocities induce larger values of the energy dissipation rate, which results in faster break-up, finer dispersions at equilibrium, and shorter residence time requirements for equilibrium.

For $n_e = 10$ and Q ranging from 204 to 600 L/h, the residence time τ varies from 0.11 to 0.04 s, where τ is defined as

$$\tau = \frac{\varepsilon V_{mixer}}{Q} = \frac{\varepsilon AL}{Q} \tag{15}$$

Note that results have been obtained with a concentration of 25% vol of dispersed phase which does not correspond to a dilute system. Such a concentration would have resulted in significant coalescence if pure liquids would have been used. However coalescence is expected to be severely hindered by the presence of the 1.5 volume percent of surfactant in the continuous phase.

3.3.3. Calculation of D_{32}: Existing Models. Different models predicting mean droplet diameters in liquid−liquid dispersions through static mixers are available in the literature. They are generally based on Kolmogorov's theory of isotropic turbulence (see Hinze[24,25]). The maximum droplet diameters depend on the turbulence fluctuations or eddies and the fluctuation velocities, and can be correlated to the mean energy dissipation rate. The most stable droplet size is thus given by:

$$D_{max} = K_1\left(\frac{\sigma}{\rho_c}\right)^{0.6}\varepsilon_v^{-0.4} \tag{16}$$

where K_1 is a dimensionless constant close to 1 and σ is the interfacial tension between the dispersed and the continuous phase.

One can note that the dispersed phase viscosity is neglected in the theory used to establish eq 16.

To take into account the viscous forces inside the drop that can contribute to break-up resistance, Davies[27] added a viscous force term to the interfacial tension and proposed:

$$D_{max} = K_2\left(\sigma + \frac{\mu_d v}{4}\right)^{0.6}\rho_c^{-0.6}\varepsilon_v^{-0.4} \tag{17}$$

where v is the turbulent eddy velocity.

According to liquid−liquid dispersion results obtained in a stirred tank, Sprow[28] assumed that D_{32} is proportional to D_{max}. As D_{max} is more difficult to determine experimentally than D_{32}, most of authors propose correlations to calculate D_{32}.

Middleman[9] proposed a correlation for noncoalescing systems in turbulent flow in a Kenics static mixer in terms of dimensionless numbers:

$$\frac{D_{32}}{D} = K_3 We_c^{-0.6} f^{-0.4} \tag{18}$$

where We_c is a dimensionless number called the Weber number defined as follows in terms of the continuous phase density and the tube diameter:

$$We_c = \frac{\rho_c V_0^2 D}{\sigma} \tag{19}$$

According to the dependency of the friction factor on the Reynolds number (see Pressure Drop in Liquid−liquid Dispersion, sec 3.2), eq 18 can be rewritten in terms of We_c and the Reynolds number:

$$\frac{D_{32}}{D} = K_4 We_c^{\alpha} Re_c^{\beta} \tag{20}$$

Where Re_c is the Reynolds number defined as a function of the continuous phase properties and the tube diameter, as follows:

$$Re_c = \frac{\rho_c V_0 D}{\mu_c} \tag{21}$$

Equation 20 is based on the superficial velocity and the housing tube diameter, and can only be applied with low-viscosity dispersed phases. Some authors like Streiff[12] defined the Reynolds and the Weber number in terms of the hydraulic diameter and the interstitial velocity. They proposed a correlation similar to eq 20, fitting both exponent values of We_h and Re_h to their experimental results. Legrand et al.[21] and Das et al.[29] also established a similar correlation to eq 20, based on the pore Reynolds number (Re_p) and the pore Weber number (We_p). Re_p and We_p depend on a porous diameter and a tortuosity factor, which are characteristic properties of the mixer.

Some authors introduced other parameters to predict the mean diameter of droplets. For example Chen and Libby[10] and Haas[30]

considered a term taking into account the viscosity ratio, and Berkman and Calabrese[11] introduced the viscosity group or capillary number V_i that represents the ratio of viscous to surface forces acting to stabilize the drop:

$$V_i = \frac{\mu_d V_0}{\sigma}\left(\frac{\rho_c}{\rho_d}\right)^{0.5} \quad (22)$$

Finally Streiff et al.[20] provided a correlation taking into consideration the dispersed phase concentration and the density ratio.

Table 3 summarizes the different correlations available and compares the respective values of α and β in eq 20. Haas[30] is the only author who reported a correlation to predict D_{43} rather than the D_{32}. D_{43} is another type of characteristic diameter corresponding to the mean volume diameter.

Except Legrand et al.,[21] Al Taweel and Chen,[15] and Das et al.,[29] all authors found exponents close to −0.6 for the Weber number. However, several authors disagree on the influence of the Reynolds number on the drop mean size. Its influence might be dependent on the flow regime as suggested by Legrand et al.:[21] under turbulent conditions, the Reynolds exponents are found to be positive; in the laminar flow regime negative exponents are obtained.

3.3.4. Relationship between D_{32} and D_{max}. Figure 15 represents D_{max} as a function of D_{32} for various numbers of SMX elements, at different flow rates. When n_e increases from 2 to 20, the ratio D_{32}/D_{max} varies from 0.33 to 0.38 (see Table 4). These results are in good agreement with the value of 0.38 obtained by Sprow[28] in a stirred tank operating in turbulent flow. The linear dependence of D_{max} with D_{32} is thus confirmed in SMX static mixers.

3.3.5. Calculation of D_{32}: Development of a Correlation for the Sauter Mean Diameter. We assumed that the best way of correlating the experimental results is to establish a relationship between the Sauter mean diameters and the mean energy dissipation rate per mass unit ε_v. Thus, in order to satisfy Kolmogorov's theory of isotropic turbulence the experimental data have been correlated as follows:

$$D_{32} = K_5 \varepsilon_v^{\ k} \quad (23)$$

Figure 16 shows values of k obtained for 2, 5, 10, 15, and 20 mixing elements. k ranges from −0.37 to −0.39 for $5 < n_e < 20$ and $k = -0.26$ for $n_e = 2$. For $n_e = 2$, the droplet size distributions are difficult to measure precisely, exhibiting a wide dispersion. In addition only three experimental data have been collected for this number of elements. As a consequence, the k value for $n_e = 2$ is questionable. For $n_e \geq 5$ experimental results are in good agreement with Kolmogorov's theory.

The pressure drops measured in the liquid−liquid dispersions showed that the friction factor is not constant in the flow rate range studied. We found that f depends on $Re_c^{-0.25}$. According to the correlation proposed by Middleman[9] (eq 18), D_{32} can be correlated as a function of We_c and Re_c, including the dependency of f versus Re_c. The following expression is obtained:

$$\frac{D_{32}}{D} = K_6 \cdot We_c^{-0.6} \cdot Re_c^{0.1} \quad (24)$$

Figure 17 shows that the experimental results are in good agreement with relation 24. However the K_6 value was found to vary between 0.19 and 0.15 depending on the value of n_e with K_6 being equal to 0.15 when equilibrium conditions are achieved. This correlation has been developed by Middleman[9] for noncoalescing systems. It is applied here to a 25% vol dispersed phase concentration system, which may involve coalescence phenomenon. But the use of a certain amount of surfactant enables coalescence to be limited.

To account for the influence of the number of elements on the mean drop size, a new term has been introduced in eq 24. Since in the range of parameters tested 10 mixing elements are needed to reach the equilibrium between breakup and coalescence, the exponent assigned to the number of elements has been determined from experimental data for 2, 5, and 10 elements. The following expression is proposed:

$$\frac{D_{32}}{D} = 0.15 We_c^{\ -0.6} Re_c^{\ 0.1} n_e^{-0.2} \quad (25)$$

Where n_e equals the real number of elements employed when $n_e \leq 10$, and n_e equals 10 when $n_e > 10$.

As can be seen on Figure 18, eq 22 fits the experimental results well for n_e ranging from 2 to 20, and Q ranging from 204 L/h to 600 L/h.

3.4. Power and Energy Dissipated: Comparison between Static Mixers and Stirred Tank. To compare the energetic efficiency of the SMX static mixer with a classical emulsification device, an additional experiment was performed in a stirred tank.

The physical characteristics of the tank are tank diameter = 0.1 m; stirrer, Rushton turbine; turbine diameter $D_t = 0.05$ m; and volume of liquid = 1 L. The stirring speed is $N = 1000$ rpm.

The comparison criterion between the stirred tank and the SMX mixer is the mean energy dissipated to reach a similar mean droplet size at the equilibrium between breakage and coalescence. The energy dissipated equals the product of the mean energy dissipation rate with the time needed to reach the equilibrium droplet size, called here the characteristic time.

It has been shown previously that this equilibrium size is reached with 10 elements for the static mixer. The characteristic time corresponds to the residence time in the mixers which depends on the working flow rate.

The time needed to reach the equilibrium in the stirred tank will be determined for the same two-phase system with the same dispersed phase concentration (25% vol).

The mean energy dissipation rate ε_v for static mixers has been previously calculated for the different flow rates studied according to relationship 14.

For stirred tanks, ε_v is calculated from the power consumption of the turbine, given by

$$P = N_p \rho_c N^3 D_t^{\ 5} \quad (26)$$

where N_p is the power number, assumed to be equal to 5.2 for Rushton turbines in turbulent flow according to Paul et al.[31]

For the stirred tank, the Reynolds number can be calculated as a function of the continuous phase properties as follows:

$$Re_{st} = \frac{\rho_c N D_t^{\ 2}}{\mu_c} \quad (27)$$

For this experiment, the Reynolds number is equal to 39000, so the flow regime is turbulent ($Re_{st} \geq 10000$). The continuous phase is introduced within the tank before starting the stirring. The dispersed phase is added quickly over the surface of the continuous phase precisely when the stirring speed reaches its permanent regime. Then stirring is maintained during 1 h.

Figure 19 shows the evolution of the Sauter mean diameter with time. D_{32} decreases quickly during the first 10 min of emulsification. Though slightly decreasing below 60 min, D_{32} remains almost constant down to 30 min. As a consequence, the time needed to reach the equilibrium size, corresponding to

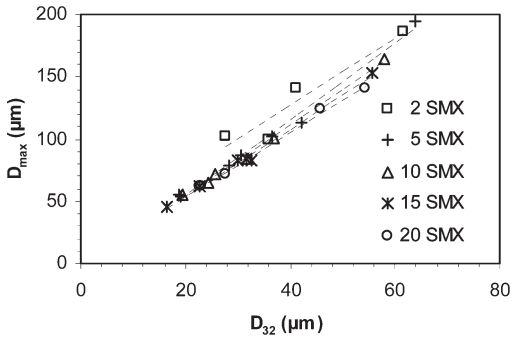

Figure 15. D_{max} versus D_{32}.

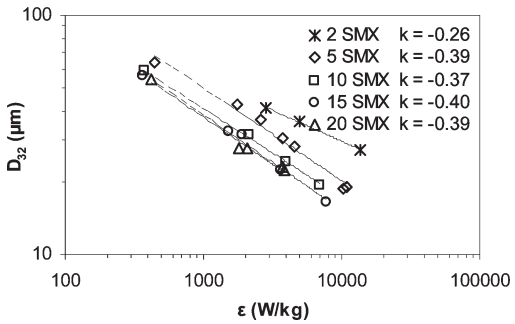

Figure 16. Effect of energy dissipation rate on the Sauter mean diameter.

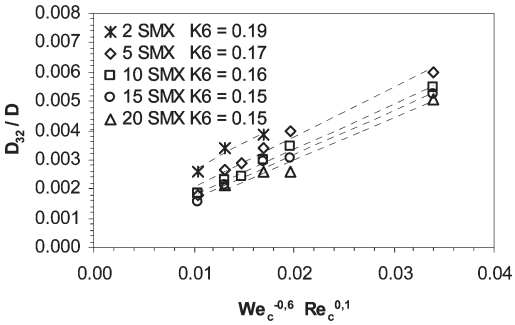

Figure 17. D_{32} versus We_c and Re_c.

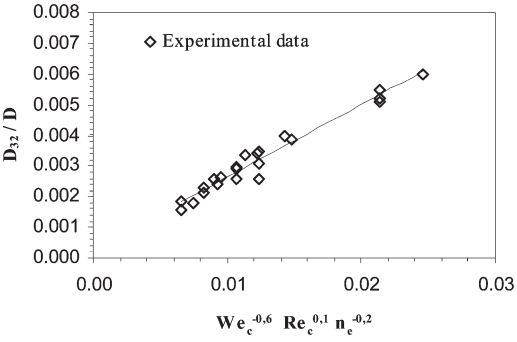

Figure 18. Comparison between experimental data and the model taking into account the number of mixing elements.

Table 4. Ratio D_{32}/D_{max} for Each Number of SMX Elements Tested

	$n_e = 2$	$n_e = 5$	$n_e = 10$	$n_e = 15$	$n_e = 20$
D_{32}/D_{max}	0.37	0.33	0.35	0.37	0.38

the chosen contact time (CT) in the stirred time is 30 min. The stabilized mean diameter equals 35 μm.

A very close value of the mean diameter ($D_{32} = 37$ μm) is obtained with the static mixers for a flow rate equal to 335 L/h. At this flow rate, the residence time in the mixers is 0.06 s.

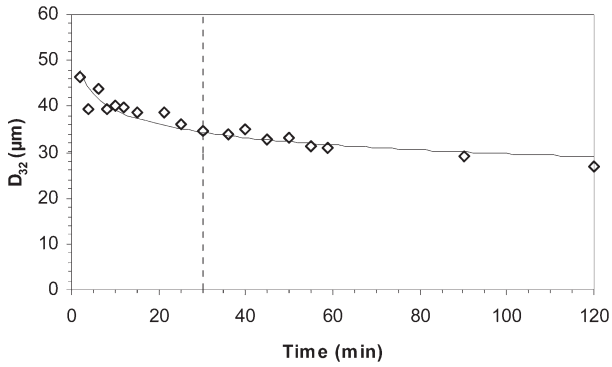

Figure 19. Evolution of the Sauter mean diameter versus time for the stirred tank experiment at 1000 rpm.

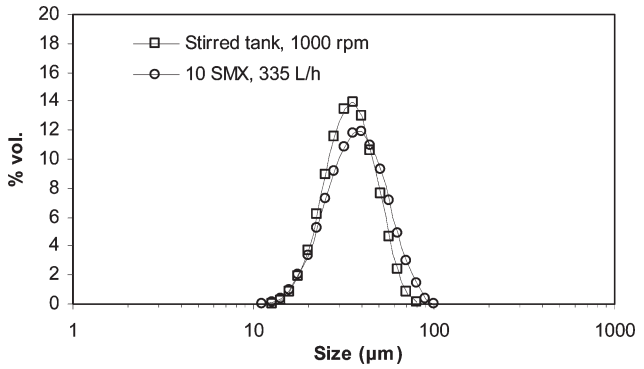

Figure 20. Comparison between the stirred tank experiment at 1000 rpm and the SMX experiment at 335 L/h with 10 elements.

Table 5. Comparison between Stirred Tank and SMX Mixers Performances in Terms of Power Needed and Energy Dissipated

device	CT or RT (s)	P(W)	ε_v (W/kg)	E (J/kg)
stirred tank	1800	7.5	8.0	14325
static mixer	0.06	9	1590	102

Figure 20 compares the equilibrium droplet size distribution obtained with both devices. They are very similar even if the distribution is slightly narrower for the stirred tank.

Table 5 gives the values of the characteristic time, the mean energy dissipation rate per mass unit, and the resulting dissipated energy for the stirred tank and the static mixer. These values show that the mean energy dissipation rate per mass unit is higher for the static mixer compared to the stirred tank ($\varepsilon_{v\ static\ mixers} = 200\varepsilon_{v\ stirred\ tank}$). As the contact time CT is far lower for the static mixer ($CT_{stirred\ tank} = 30000CT_{static\ mixer}$), this leads to a lower energy dissipated for the static mixer than for the stirred tank.

Static mixers dissipate energy more uniformly than stirred tanks, and all droplets are exposed to fairly uniform shear stress as they pass through the media. In stirred tanks, the energy is focused at the trailing vortices behind the blades of the turbine. The time needed to reach the equilibrium between break up and coalescence in the stirred tank is rather long, typically about 30 min in our case instead of 0.06 s in SMX mixers. As a consequence, the mean energy dissipated per mass unit, which truly represents the energy cost of the operation, is much lower for the static mixer than for the stirred tank equipped with a Rushton turbine.

4. Conclusion

The pressure drop for single-phase and two-phase flows and the droplet size of emulsions under turbulent flow with a Sulzer

SMX static mixer have been investigated in a wide range of parameters. The geometric and hydrodynamic parameters considered are the number of mixing elements and the fluid flow rate.

A correlation based on the Blasius' equation is established to model the pressure drop in single-phase flow in the turbulent flow regime. The transition between the transient and turbulent flow regimes occurs around *Re* equal to 800.

The discrepancies between the parameters of our model and those found in the literature are explained by the geometric characteristics of the mixers, in particular their porosity.

Pressure drops in two phase flow are successfully predicted by the correlation established for single-phase flow.

Liquid−liquid dispersion experiments in turbulent flow with different numbers of mixer elements allowed us to determine the number of mixing elements needed to reach the equilibrium between breakage and coalescence.

We conclude that Kolmogorov's theory of isotropic turbulence is valid to predict the mean droplet size. A correlation taking into account the Weber and Reynolds numbers and the number of mixing elements is established to calculate the Sauter mean diameter under turbulent flow.

Finally the power and energy dissipated are calculated for the same operation in both the stirred tank and the SMX mixer. This allows the economic interest of the SMX mixer to be quantified. The energy dissipated per mass unit, i.e., the energy cost of the operation, is lower for the static mixer than for the stirred tank equipped with a Rushton turbine. The static mixer is thus an economic alternative to the stirred tank for continuous emulsification processes.

Acknowledgment

Technical support of this work from Sulzer Chemtech AG, Winterthur, is gratefully acknowledged. The authors thank Dr. Philip Nising for his comments in the elaboration of this work.

Literature Cited

(1) Shah, N. F.; Kale, D. D. Pressure drop for laminar flow of non-Newtonian fluids in static mixers. *Chem. Eng. Sci.* **1991**, *46*, 2159.

(2) Yang, H. C.; Park, S. K. Pressure drop in motionless mixers. *Korean Soc. Mech. Eng. Int. J.* **2004**, *18*, 526.

(3) Li, H. Z.; Fasol, C.; Choplin, L. Pressure drop of Newtonian and non-Newtonian fluids across a Sulzer SMX static mixer. *Trans. IChemE* **1997**, *75 A*, 792.

(4) Pahl, M. H.; Muschelknautz, E. Einsatz und Auslegung statisher Mischer. *Chem. Ing. Technol.* **1979**, *51*, 347.

(5) Pahl, M. H.; Muschelknautz, E. Statische Mischer und ihre Anwendung. *Chem. Ing. Technol.* **1980**, *52*, 285.

(6) Pahl, M. H.; Muschelknautz, E. Static Mixers and their applications. *Int. Chem. Eng.* **1982**, *22*, 197.

(7) Bohnet, M.; Kalbitz, H.; Nemeth, J.; Pazmany, J. Improvement of forced convection heat transfer by using static mixers. *Proc. Int. Act. Conf., INTC Jerusalem* **1990**, 315.

(8) Streiff, F. A. ; Jaffer, S.; Schneider, G. The design and application of static mixer technology. 3rd International Symposium on Mixing in Industrial Processes, Osaka, Japan, 1999; p 107.

(9) Middleman, S. Drop size distributions produced by turbulent pipe flow of immiscible fluids through a static mixer. *Ind. Eng. Chem. Process Des. Develop.* **1974**, *13*, 78.

(10) Chen, S. J., Libby, D. R.; Gas−liquid and liquid−liquid dispersions in a Kenics mixer. 71st Annual AIChE Meeting, Miami, FL, 1978.

(11) Berkman, P. D.; Calabrese, R. V. Dispersion of viscous liquids by turbulent flow in a static mixer. *AIChE J.* **1988**, *34*, 602.

(12) Streiff, F. In-line dispersion and mass transfer using static mixing equipment. *Sulzer Technol. Rev.* **1977**, 108.

(13) Matsumura, K.; Morishima, Y.; Masuda, K.; Ikenaga, H. Some performance data of the Hi-mixer—An in-line mixer. *Chem. Ing. Technol.* **1981**, *53*, 51.

(14) Al Taweel, A. M.; Walker, L. D. Liquid dispersion in static in-line mixers. *Can. J. Chem. Eng.* **1983**, *61*, 527.

(15) Al Taweel, A. M.; Chen, C. A novel static mixer for the effective dispersion of immiscible liquids. *Trans IchemE.* **1996**, *74*, 445.

(16) Lemenand, T.; Zellouf, Y.; Della Valle, D.; Peerhossaini, H. Formation de gouttelettes dans un mélange turbulent de deux fluides immiscibles (Droplet formation in the turbulent mixing of two immiscible fluids). *15ème Congr. Fr. Méc.* **2001**, 494.

(17) Lemenand, T.; Della Valle, D.; Zellouf, Y.; Peerhossaini, H. Droplets formation in turbulent mixing of two immiscible fluids in a new type of static mixer. *Int. J. Multiphase Flow* **2003**, *29*, 813.

(18) Lemenand, T.; Dupont, P.; Della Valle, D.; Peerhossaini, H. Turbulent mixing of two immiscible fluids. *Trans. Am. Soc. Mech. Eng.* **2005**, *127*, 1132.

(19) Yamamoto, T.; Kawasaki, H.; Kumazawa, H. Relationship between the dispersed droplet diameter and the mean power input for emulsification in three different types of motionless mixers. *J. Chem. Eng. Jpn.* **2007**, *40*, 673.

(20) Streiff, F. A.; Mathys, P.; Fischer, T. U. New fundamentals for liquid−liquid dispersion using static mixers. *Réc. Progr. Génie Proc.* **1997**, *11*, 307.

(21) Legrand, J.; Morancais, P.; Carnelle, J. Liquid−liquid dispersion in an SMX-Sulzer static mixer. *Inst. Chem. Eng.* **2001**, *79, Part A*, 949.

(22) Hirschberg, S.; Koubek, R.; Moser, F.; Schöck, J. An improvement of the Sulzer SMX static mixer significantly reducing the pressure drop. *Chem. Eng. Res. Des.* **2009**, *87*, 524.

(23) Thakur, R. K.; Vial, C.; Nigam, K. D. P.; Nauman, E. B.; Djelveh, G. Static mixers in the process industries—A review. *Trans. IChemE* **2003**, *81*, 787.

(24) Hinze, J. O. *Turbulence*; McGraw-Hill: New York, 1959; p 183.

(25) Hinze, J. O. Fundamentals of the hydrodynamic mechanism of splitting in dispersion processes. *AIChE J.* **1955**, *1*, 289.

(26) Rama Rao, N. V.; Baird, M. H. I.; Hrymak, A. N.; Wood, P. E. Dispersion of high-viscosity liquid−liquid systems by flow through SMX static mixer elements. *Chem. Eng. Sci.* **2007**, *62*, 6885.

(27) Davies, J. T. Drop sizes of emulsions related to turbulent energy dissipation rates. *Chem. Eng. Sci.* **1983**, *40*, 839.

(28) Sprow, F. B. Distribution of drop sizes produced in turbulent liquid−liquid dispersion. *Chem. Eng. Sci.* **1967**, *22*, 435.

(29) Das, P. K.; Legrand, J.; Morançais, P.; Carnelle, G. Drop breakage model in static mixers at low and intermediate Reynolds number. *Chem. Eng. Sci.* **2005**, *60*, 231.

(30) Haas, P. A. Turbulent dispersion of aqueous drops in organic liquids. *AIChE J.* **1987**, *33*, 987.

(31) Paul, E. L.; Aatiemo-Obeng, V.; Kresta, S. M. *Handbook of Industrial Mixing: Science and Practice*; Wiley: New York, 2003; p 1351.